Acta Mech 231, 3031–3042 (2020)
https://doi.org/10.1007/s00707-020-02691-x

ORIGINAL PAPER

Sharadwata Pan · Natalie Germann

Mechanical response of industrial benchmark lipsticks under large-scale deformations

Received: 22 December 2019 / Revised: 19 February 2020 / Published online: 16 May 2020

Abstract This work documents the first account of advanced mechanical properties of six commercial lipsticks, some of which serve as market leads. We systematically studied their nonlinear viscoelastic properties under large amplitude oscillatory shear deformations. At large strains, all lipsticks showed intercycle strain softening, the extent of which initially depended on the prototype in the nonlinear regime. This behavior, markedly, was absent after the crossover of the dynamic moduli. Parameters obtained from the strain amplitude sweeps, i.e., the intrinsic elastic modulus and the stress maximum, demonstrated distinct prototype dependence. The Lissajous plots and the dimensionless nonlinear indices were determined using the MITlaos software. They showed intracycle elastic strain stiffening and viscous shear thinning. The angular oscillation frequency directly influenced the linear viscoelastic measures of all the benchmark lipsticks, and the nonlinear properties of only a few benchmark ones. The current study generates standard nonlinear rheology data that can be associated with the lipstick sensory attributes and typical tribological parameters. This may serve as an effective way to examine the transition from the initial spreading to the post-application sensation.

1 Introduction

The current generation of commercially procurable lipsticks requires suitable mechanical characteristics to generate superior features, both in terms of market coverage and customer acceptance. For instance, a lipstick must show an extended shelf-life and steadiness against humidity and temperature (55–75 °C), provide dermatological protection, should be devoid of physical artifacts including sweating and fissures, possess an amiable fragrance and taste, show easy melting at the lip temperature (32 °C), coupled with substantial spreadability and wearability [1–3]. The lipstick viscosity has to be high enough to hold its structure in the mold. Furthermore, it should gradually decrease as the mechanical stress is increased during the physiological application [3]. From a tribological perspective, lipsticks necessitate different degrees of friction to slither effortlessly over skin [4]. This assists in regulating applications like sweating. The wearing rate should be enough to leave a transfer film, but not so extreme that the film is objectionably impenetrable. These perceptions are expedited by an improved understanding of the real material properties under industrial production settings. There is also a direct or indirect influence on the customer base, which can vary widely based on climate, location, culture, and perceptibility.

Past rheological investigations on organogels, wax-based emulsions, waxy crude oils, and lipstick formulations have shown the effectiveness of rheological characterizations in explaining their mechanical properties

S. Pan · N. Germann (✉)
Fluid Dynamics of Complex Biosystems, School of Life Sciences Weihenstephan, Technical University of Munich, 85354 Freising, Germany
E-mail: natalie.germann@tum.de

S. Pan
E-mail: sharadwata.pan@tum.de

[4–10]. Very recently, we systematically characterized the small amplitude oscillatory shear (SAOS) rheological properties of a wide range of commercially accessible industrial-grade lipsticks and related them with their thermal profiles [11]. We recorded the dynamic moduli, the strain-independent linear viscoelastic (LVE) regime, strain softening at high strains, appreciable inherent elasticity, and the bulk melting point, amongst others. We found that the viscoelastic characteristics of all benchmark lipsticks are governed by a predominant elastic contribution. Additionally, the lipsticks possess distinct magnitudes of intrinsic elasticity at the limit of zero deformation, as well as different extents of strain tolerating abilities in the LVE regime. More importantly, we associated the rheological quantities with indicative textural features and categorized them according to customer groups. We noted that there is no lipstick offering the supreme characteristic on every account. Instead, the thermomechanical parameters need to be customized depending on the customer base.

Large amplitude oscillatory shear (LAOS) technique conveys a way to vigorously investigate the mechanical distortions of a soft solid microstructure under large deformations, both under stress-controlled and strain-controlled modes [12–15]. Several strategies were reported for analyzing the LAOS data, which present a distinct evolutionary pattern. The high-resolution Fourier transform (FT) rheology was the foremost, which was considered as the state of the art for a considerable period [16,17]. Although the FT analysis presented quantitative information, interpretations in terms of mechanical terminologies could not be enforced. This limitation motivated McKinley and coworkers to extend the stress decomposition method proposed by Cho et al. [18], leading to the well-known Chebyshev approach [13,19,20]. The nonlinear response could be more stringently characterized compared to step inputs, i.e., creep tests and start-up of steady shear. Also, experimental artifacts such as edge fracture could be evaded in stress-controlled rheometers [13]. However, the approach also has its limitations [15,21,22]. For instance, the extraordinarily severe symmetry assumptions often lead to confusion when it comes to data interpretations. It is ambiguous how the outcomes from the static or time-averaged analysis patterns can be associated with different examination methods. The LAOStrain framework with the total strain does not guarantee the linearity of the time-decayed response and cannot explain the stress overshoots [12]. These problems led to recent advancements, highlighting the significance of the dynamic or instantaneous nonlinear viscoelastic response. The transient response facilitates the interpretations of different microstructural states under quasilinear LAOS deformations [23]. More recently, using a sequence of physical progress or SPP scheme, a full set of time-dependent viscoelastic parameters was defined, explained, and compared with experiments [15]. As demonstrated, it advances the knowledge of thixotropy, yielding, and other advanced structure-property relationships under large-scale deformations [24–26]. During topical cosmetic product applications, the typical shear rates can reach staggering magnitudes of $10^3-10^4\ s^{-1}$ [27,28]. This necessitates investigations of such materials under large-scale deformations.

Past studies have rheologically characterized lipstick formulations and other cosmetic products at large strains or very high shear rates, based on inelastic behavior and transient material properties [29,30]. Pénzes et al. [29] predicted structural information, network elasticity, and crosslinking energy by carrying out nonlinear oscillatory stress sweeps of pharmaceutical-grade organogels. Goik et al. [7] showed that rheological additives, for instance, propolis, do not affect lipstick viscoelasticity. Besides, the apparent viscosity profoundly influences the lipstick usage parameters, such as the contact time with the skin. Ozkan et al. [30] used conventional and FT rheology to characterize the stress tolerance of skin and hair gels under steady torsional flow, uninterrupted shear-rate ramps, extensions, and dynamic LAOS stresses. The authors associated these properties with sensory features and reported that thixotropy and wall slip greatly affect the product spreadability. Particularly, LAOS was shown to be instrumental in comprehending the investigation of sensorial aspects. Using rotational rheometry, oscillatory shear rheology, and creep compliance studies, Haj-shafiei et al. [31] showed that the development of wax crystals restricts the breakdown of W/O emulsions induced by shearing deformations, which would negatively impact their spreadability. Tribological studies of cosmetic samples were also carried out. Timm et al. [32] demonstrated that the overall friction could be reduced by cosmetic polymer particles, their particle size being a controlling parameter. The frictional standards of different moisturizers, i.e., solids suspended in liquids, were associated with sensory parameters like stickiness and spreading, based on trained sensory panel assessments [33]. Beri [4] systematically studied the effects of disk speed and normal force on friction and wear for a variety of solid wax-based emulsions. The friction coefficient was shown to increase with increasing wax concentration, droplet size, and aqueous volume proportion. Additionally, friction was found to be an effective tribological indicator for the smoothness of a lipstick formulation [4].

Despite these developments in the rheological characterization of cosmetic emulsions and lipstick formulations, there are scopes for further investigations. To our knowledge, there is no systematic investigation of the nonlinear viscoelastic parameters of commercial benchmark lipsticks under LAOS stresses. Such a study can explore the relationship between the maximum stress tolerance and the inherent elastic potential. It will also

Table 1 Industrial benchmark (BM) lipsticks examined in this work

Sample code	Benchmark lipstick trade name
BM-1	Labello® Original
BM-2	Natural ingredient-based formulation (KHK, GmbH)
BM-3	Bepanthol®
BM-4	Weleda EVERON®
BM-5	BURT'S BEES HONEY®
BM-6	eos® Organic Strawberry Sorbet

clarify the influence of the strain on the destructive behavior of the wax crystal network. Furthermore, it can also help to categorize the customers based on the qualitative trends of the advanced mechanical parameters. The objective of the present study is to systematically investigate these aspects by studying the qualitative nonlinear rheological trends of our benchmark lipsticks under LAOS stresses. The article is arranged as per the following segments. Section 2 briefly explains the benchmark lipstick sample set, the experimental methodology, and data analysis procedures. In Sect. 3, we present the principal outcomes from the current work. Section 4 discusses these results and puts them into contexts. Finally, we summarize the key inferences in Sect. 5.

2 Materials and methods

2.1 Commercial benchmark lipsticks

We investigated the nonlinear rheology of six industrial lipsticks, as listed in Table 1. BM-1 and BM3–BM-6 were purchased from well-known online retailers in Germany. BM-2 was contributed by KHK GmbH (Cologne, Germany) purely for scientific investigation purposes. The precise list and proportions of the lipstick constituents, as well as the industrial preparation and filling procedures, were outside the capacity of the current investigation, because of individual company regulations. The choice of these particular lipstick prototypes has already been rationalized in our recent article [11], which used the same lipstick prototypes as herein. Briefly, we considered the extent of their market spread (both online and in the real market), consumer suitability in a specific country (like Germany) or continent (Europe and USA), future incorporation of novel natural ingredients (e.g., BM-2), amongst others. We did not categorize the prototypes based on formulation type, texture, color, fragrance, or any other related parameter.

2.2 Oscillatory shear rheology

We used a standard Physica MCR 502 rheometer with a smooth, stainless steel parallel plate geometry (Anton Paar, Graz, Austria) for the oscillatory shear measurements. The stress-controlled rheometer was utilized in the strain-controlled mode for the rheological characterizations. Critically, the direct strain oscillation or DSO selection of the instrument was employed to safeguard an accurate sinusoidal strain at all imposed amplitudes. Several researchers have successfully carried out LAOS experiments with a stress-controlled rheometer and have reported the nonlinear viscoelastic responses for a wide range of samples [34,35]. The diameters of the top and bottom plates were 8 and 15 mm, respectively. To circumvent sample slippage, we covered the plates with sandpapers using double-adhesive tapes. We maintained the gap at 0.7 mm, irrespective of the sample and rheometric protocol. We carried out all tests at the lip physiological temperature of 32 °C. To verify the reproducibility of our results, we tested multiple samples corresponding to each brand. More details about the step-wise sample preparation, the temperature and moisture regulation, as well as the sample loading, and normal force monitoring procedures are given in our recent lipstick article [11]. The supplementary information (SI) file of the corresponding article also provides a pictorial representation of the measuring system (see Fig. S2). The principal measurement performed in this study was that of an isothermal strain sweep extending from SAOS to LAOS strains ($0.001 < \gamma < 100\%$), at a fixed angular oscillation frequency ($10\,\mathrm{rad\,s^{-1}}$) to identify the LVE and nonlinear regimes, respectively. We simultaneously recorded the intracycle waveforms at each strain amplitude and subsequently analyzed them as described in Sect. 2.3. To examine the intracycle linear viscoelastic behaviors, we carried out frequency sweeps at fixed low strains ($0.02 < \gamma < 0.5\%$).

2.3 LAOS data interpretation using MITlaos

We interpreted the stress waveforms recorded at 10 rad s^{-1} and distinct strain amplitudes using the MITlaos software platform (Ver. 2.2 Beta, MATLAB). For comparison purposes, we also analyzed the strain sweep data obtained for the same lipsticks at 1 rad s^{-1} reported in our recent study [11]. We qualitatively analyzed the nonlinear stress response via elastic and viscous Lissajous–Bowditch curves. To study the LVE regime, we first determined the first harmonic elastic (G_1') and viscous (G_1'') moduli and verified its identical magnitudes with the linear storage and loss moduli, respectively, across the entire strain range. To study the storage of the elastic energy at large deformations, we estimated the nonlinear elastic moduli [20]

$$G'_{\mathrm{M}} \equiv \left.\frac{\mathrm{d}\sigma}{\mathrm{d}\gamma}\right|_{\gamma=0} = e_1 - 3e_3 + \cdots, \tag{1}$$

and

$$G'_{\mathrm{L}} \equiv \left.\frac{\sigma}{\gamma}\right|_{\gamma=\pm\gamma_0} = e_1 + e_3 + \cdots. \tag{2}$$

Here, G'_{M} is the minimum strain or tangent modulus at the maximum shear rate or the minimum strain ($\gamma = 0$), and G'_{L} is the large strain or secant modulus at the minimum shear rate or the maximum strain ($\gamma = \pm\gamma_0$). Further, σ denotes the shear stress, γ_0 is the strain amplitude, and e_1 and e_3 represent the first-order and third-order elastic Chebyshev coefficient, respectively. Finally, we quantitatively analyzed the nonlinear response in terms of the strain stiffening (S) and shear thickening (T) ratios, expressed as [20]:

$$S \equiv \frac{G'_{\mathrm{L}} - G'_{\mathrm{M}}}{G'_{\mathrm{L}}} = \frac{4e_3 + \cdots}{e_1 + e_3 + \cdots}, \tag{3}$$

and

$$T \equiv \frac{\eta'_{\mathrm{L}} - \eta'_{\mathrm{M}}}{\eta'_{\mathrm{L}}} = \frac{4v_3 + \cdots}{v_1 + v_3 + \cdots} \tag{4}$$

In Eq. (4), η'_{M} and η'_{L} denote the local viscosities at the minimum and maximum strain, respectively, and v_1 and v_3 represent the first-order and third-order viscous Chebyshev coefficient, respectively. In a recent article, these dimensionless indices were found to exhibit a stronger nonlinear response than the Chebyshev ratios [35]. Only $\sim$ 25% of the entire nonlinear influence on the LAOS stress is incorporated in e_3 and v_3, and hence, it is not sufficient to only consider the Chebyshev coefficients or their ratios [20]. LAOS studies have already been extensively carried out in our group, and the applied analysis procedures were explained in great detail in our previous works [35–37].

3 Results

Figure 1a displays a representative full mechanical spectrum in terms of the strain amplitude sweep of BM-1 performed at $\omega = 10$ rad s^{-1}. The qualitative trends of the LVE moduli for the other benchmark lipsticks are similar to the one shown in Fig. 1a, as well as to the ones obtained previously at $\omega = 1$ rad s^{-1} [11]. Namely, we find predominant elastic contributions to viscoelasticity ($G' > G''$) in the LVE region, which is dependent on the benchmark prototype. In the LAOS region, we see strain softening, followed by a crossover of the dynamic moduli. However, the magnitudes of the LVE moduli reported here, i.e., at $\omega = 10$ rad s^{-1}, are larger compared to the ones observed in our previous study at $\omega = 1$ rad s^{-1}. Quantitatively, the moduli magnitudes at $\omega = 10$ rad s^{-1} can be broadly categorized into two distinct groups. BM-2, BM-3, and BM-5 represent the larger cohort, while the rest characterizes the smaller unit. The behaviors of the nonlinear viscoelastic moduli are discussed later. The evolution of the shear stress amplitude as a function of the strain amplitude (Fig. 1b) shows similar qualitative trends as in our previous study [11]. For instance, we observe a power-law region in the LVE regime until the onset of nonlinearity. We define this onset as where the strain amplitude in the strain sweep deviates from the linear viscoelastic regime. Although not explicitly displayed here, it may be noted that the LVE strain amplitude limits of BM-4 and BM-6 are not much higher than those of the other specimens, indicating similar deformation tolerability. We also carried out frequency sweeps at chosen strain amplitudes within the LVE regime (Fig. 1c). We see typical semi-solid behaviors, with a dominant elastic contribution

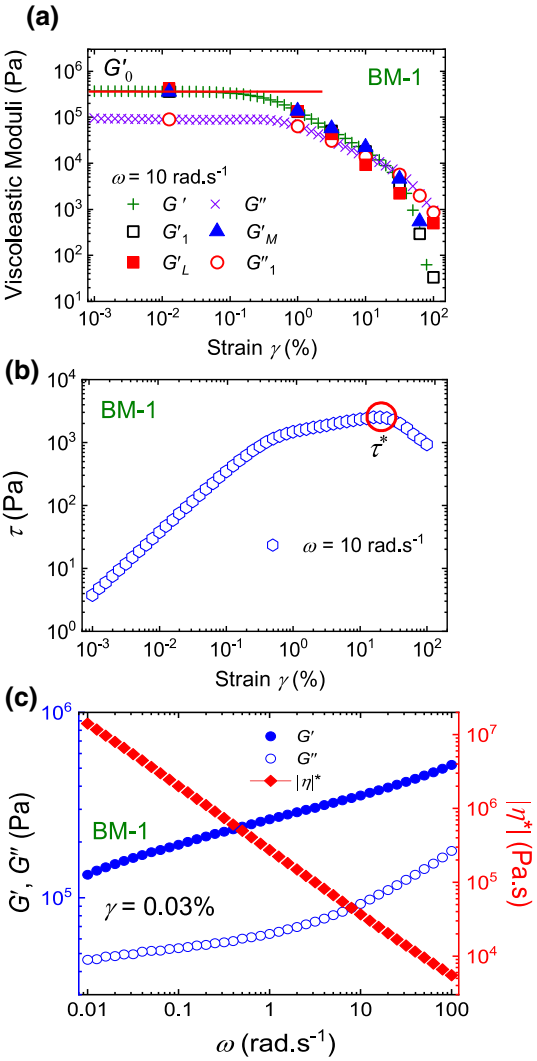

Fig. 1 **a** Representative strain sweep data of benchmark lipstick BM-1, showing linear elastic (G') and viscous (G'') moduli and nonlinear moduli (G'_1, G'_M, G'_L, G''_1) as a function of strain amplitude, γ, at angular frequency of $\omega = 10\,\mathrm{rad\,s^{-1}}$. G'_0 is the intrinsic elastic modulus, indicating the elastic potential in an undistorted state. **b** Evolution of shear stress amplitude, τ, as a function of strain amplitude γ, during strain sweep of BM-1. τ^* (hollow circle) denotes the stress maximum. **c** Frequency sweep of BM-1 displaying evolution of G' (filled circles), G'' (open circles) and complex viscosity η^* (filled diamonds) in LVE regime at $\gamma = 0.03\%$. All experiments were carried out at a temperature of 32 °C

to linear viscoelasticity. The complex viscosity does not reach a plateau even at an angular frequency of 0.01 rad s^{-1}. The relaxation time could not be estimated as the dynamic moduli did not exhibit a crossover in the probed frequency range. These observations hold for all lipsticks.

We used two additional parameters, namely, the intrinsic elastic modulus, G'^0, and the shear stress maximum, τ^*. As illustrated in Fig. 1a, G'_0 was obtained by extrapolating the strain amplitude dependence of G' at the limit of zero strain through least-squares linear fitting with a slope equal to zero. As indicated in Fig. 1b, τ^* was obtained from the strain amplitude sweep, representing the maximum value of the shear stress amplitude. The estimated parameters are displayed for the different benchmark lipsticks in Fig. 2a, b, respectively. The qualitative trends of τ^* and G'_0 are not identical, although both are prototype dependent. For instance, Fig. 2a shows that BM-4 demonstrates the highest stress tolerance (8–12 kPa), followed by BM-2 (3–6 kPa) and BM-5 (3–5 kPa). On the other hand, the mean values indicate that BM-1 and BM-6 are the least capable of withstanding a high shear stress ($\sim$ 2 kPa). From Fig. 2b, as noted earlier, we find that the values of G'_0 can be loosely categorized into two main groups. While BM-2, BM-4, and BM-5 represent the larger cohort in terms of magnitude (700–1000 kPa), BM-1, BM-3, and BM-6 constitute the smaller unit (300–500 kPa).

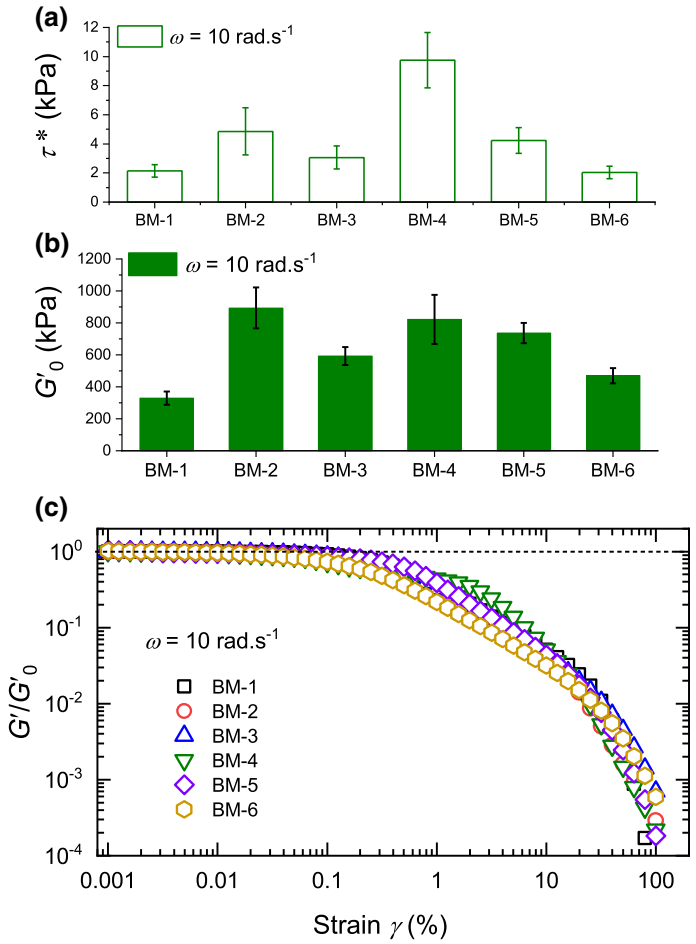

Fig. 2 Strain-sweep measures calculated for different benchmark lipsticks, as illustrated in Fig. 1. **a** Maximum shear stress amplitude, τ^*, and **b** zero-strain or intrinsic elastic modulus, G'_0. **c** Intercycle elastic response of benchmark lipsticks in terms of dimensionless elastic modulus, G'/G'^0, across the entire strain amplitude range from LVE to nonlinear regimes. The characteristics in (**a**, **b**) represent the mean of at least five samples. The error bars indicate standard deviations. The sample codes are explained in Table 1

Undoubtedly, BM-1 possesses the lowest G'_0 value (300–350 kPa) at the undistorted state. Comparing the G'_0 values obtained at $\omega = 10\,\mathrm{rad\,s^{-1}}$ (current study) with the ones obtained at $\omega = 1\,\mathrm{rad\,s^{-1}}$ [11], we note that the zero-strain elastic modulus increases with increasing angular frequency. A non-dimensional representation of the intercycle elastic strain softening is shown in Fig. 2c, where we used G'_0 to non-dimensionalize the elastic moduli across all strains. The degree of strain softening depends on the lipstick prototype. It appears over almost two orders of magnitude of strains ($0.2\% < \gamma < 20\%$) in the nonlinear regime, corresponding to the region before the crossover of the dynamic moduli (Fig. 1a). After the crossover ($\gamma > 20\%$), however, all lipsticks seem to follow a universal behavior, with an identical terminal slope. The effectiveness of using such types of measures was already demonstrated in some of our earlier studies [11,35,38].

Figure 3 shows the representative viscous (instant stress vs. instant strain rate) and elastic (instant stress vs. instant strain) Lissajous curves of BM-5 at distinct values of imposed strain amplitudes at $\omega = 10\,\mathrm{rad\,s^{-1}}$. For comparison purposes, we also present the curves at $\omega = 1\,\mathrm{rad\,s^{-1}}$, which we extracted from the strain amplitude sweeps presented in our recent study [11]. In each curve, the solid line represents the total stress. The broken line represents the decomposed elastic or viscous stress, depending upon the elastic energy storage or viscous dissipation, respectively. The qualitative trends of the Lissajous curves were identical, irrespective of the lipstick prototype (data not shown). Namely, at the smallest strain amplitude values ($\gamma = 0.1$ and 0.316%), the LVE regime is evident from the elliptical configurations with two mirror planes. The onset of nonlinearity is prototype-dependent and occurs for BM-5 at an approximate strain amplitude of 0.63%. As the strain is further increased, i.e., at strain amplitudes of 1, 3.16, 6.31, and 10%, both the elastic and viscous stress contributions

become increasingly nonlinear, as validated by the distorted curve conformations. All lipsticks show distinct intracycle elastic strain hardening and intracycle viscous shear thinning. In addition to the unique shapes, the multiple deviations in the slopes (broken dashed lines in Fig. 3) corroborate these trends. We do not see a significant impact of the oscillation frequency on the shapes of the Lissajous curves up to a strain amplitude of 10%. Quantitative differences are reflected in the magnitudes of maximum and minimum instantaneous stress responses at 6.31%, as well as in the LVE regimes in Fig. 3, where the viscoelastic stress magnitudes at $\omega = 10\,\mathrm{rad\,s^{-1}}$ (columns C and D) are double compared to the ones at $\omega = 1\,\mathrm{rad\,s^{-1}}$ (columns A and B). These results were quantified using additional elastic nonlinear parameters, the outcomes of which are presented in the following two Subsections.

A deeper insight into the contributions of the higher-order odd harmonics can be obtained by quantifying the mechanical response in terms of nonlinear viscoelastic moduli and their ratios [13]. We first compare the intercycle behaviors of these nonlinear viscoelastic moduli for BM-1 with the LVE moduli across the entire strain range (Fig. 1a). The first harmonic elastic (G'_1, hollow squares) and viscous (G''_1, hollow circles) moduli overlap with G' and G'', correspondingly, as anticipated. The quantification of the nonlinear response, especially in terms of the elastic energy storage, is represented by the minimum strain or tangent modulus, G'_M, at $\gamma = 0$ and the large strain or secant modulus, G'_L, at the maximum applied deformation ($\gamma = \pm\gamma_0$). Similarly, two local viscosities, i.e., η'_M at zero strain and η'_L at the maximum strain, can be considered, representing identical connotations corresponding to their elastic counterparts. In the lipstick-dependent LVE regime, we observe $G'_1 = G'_M = G'_L = G'$, in agreement with theoretical postulations [20]. In the nonlinear regime, G'_M and G'_L exhibit unique trends at high strains. While the magnitudes of both nonlinear elastic moduli appear to diminish with increasing strain amplitudes, G'_M decreases at a comparatively higher rate than G'_L. The rate of decrease in G'_M is also higher for the higher oscillation frequency. Although not shown here, an analogous drift was noted for η'_M and η'_L. This is an additional validation of the intercycle strain-softening tendency during the viscous stress decay.

Figure 4 quantifies the strain dependence of the intracycle viscoelastic response in terms of the dimensionless indices of nonlinearity. The strain-stiffening and shear-thickening ratios are defined as $S \equiv (G'_L - G'_M)/G'_L$ and $T \equiv (\eta'_L - \eta'_M)/\eta'_L$, respectively [20]. In the LVE regime ($< 1\%$ strain amplitude), we obtain $S \approx 0$ and $T \approx 0$ irrespective of the lipstick type, as anticipated. At 0.01% strain amplitude, there are a few cases with $S < 0$ and $T > 0$ (not shown here). This does not signify intracycle elastic strain-softening and viscous shear-thickening behaviors, but rather noisy signals at such low deformations. With a gradual progression into the nonlinear regime, i.e., between 1 and 10% strain amplitude, we observe $S > 0$ and $T < 0$. This suggests intracycle elastic strain stiffening and viscous shear-thinning behaviors. For BM-2, the quantitative elastic response is stronger at the higher oscillation frequency of $\omega = 10\,\mathrm{rad\,s^{-1}}$, as revealed by the magnitude of S. However, the direct influence of a higher oscillation frequency on S is only valid at the strain amplitude of 10% for BM-5 and BM-6, but not true for the other benchmark lipsticks. As for T, we observe two main trends. There is not a noteworthy influence of a higher oscillation frequency on T for BM-1, BM-4, and BM-5, although some dependence of the same on T could be noted for the other lipsticks, however, only at the strain amplitude of 10%. Prior to intracycle shear thinning, we see no noticeable shear-thickening trends for any lipstick.

4 Discussion

In this work, we deal with two types of mechanical responses. Figure 1a and b shows the evolution of the dynamic moduli or stress amplitude as a function of the strain amplitude. This is an intercycle response as it occurs across cycles of different maximum imposed strain amplitudes. The Lissajous plots in Fig. 3, however, display an intracycle response, i.e., it occurs within one stress–strain curve cycle as the instantaneous strain oscillates between the minimum and the maximum imposed strain amplitude. The intercycle strain-softening behavior of the commercial lipsticks (Fig. 1a) corresponds to Type I LAOS behavior [19]. This is also in agreement with previous observations on organogels [5] and lipsticks [7,8,11]. Type I LAOS behavior is characteristic of a variety of systems, including entangled synthetic polymer systems [36,39], biopolymer and injectable hydrogels [37,40], native biological tissues [35,41,42], and food hydrocolloids [43–45]. At 0.03% strain amplitude, the frequency sweep data of BM-1 show that $G' > G''$ (Fig. 1c), conveying the robustness of the physical network [28]. This predominant elastic contribution to the linear viscoelastic response is a hallmark of all benchmark lipsticks tested in this work.

Additional information can be obtained from the calculated strain amplitude sweep measures (Fig. 2). The energy of the crystal network of organogels is influenced by their elastic moduli, which, in combination

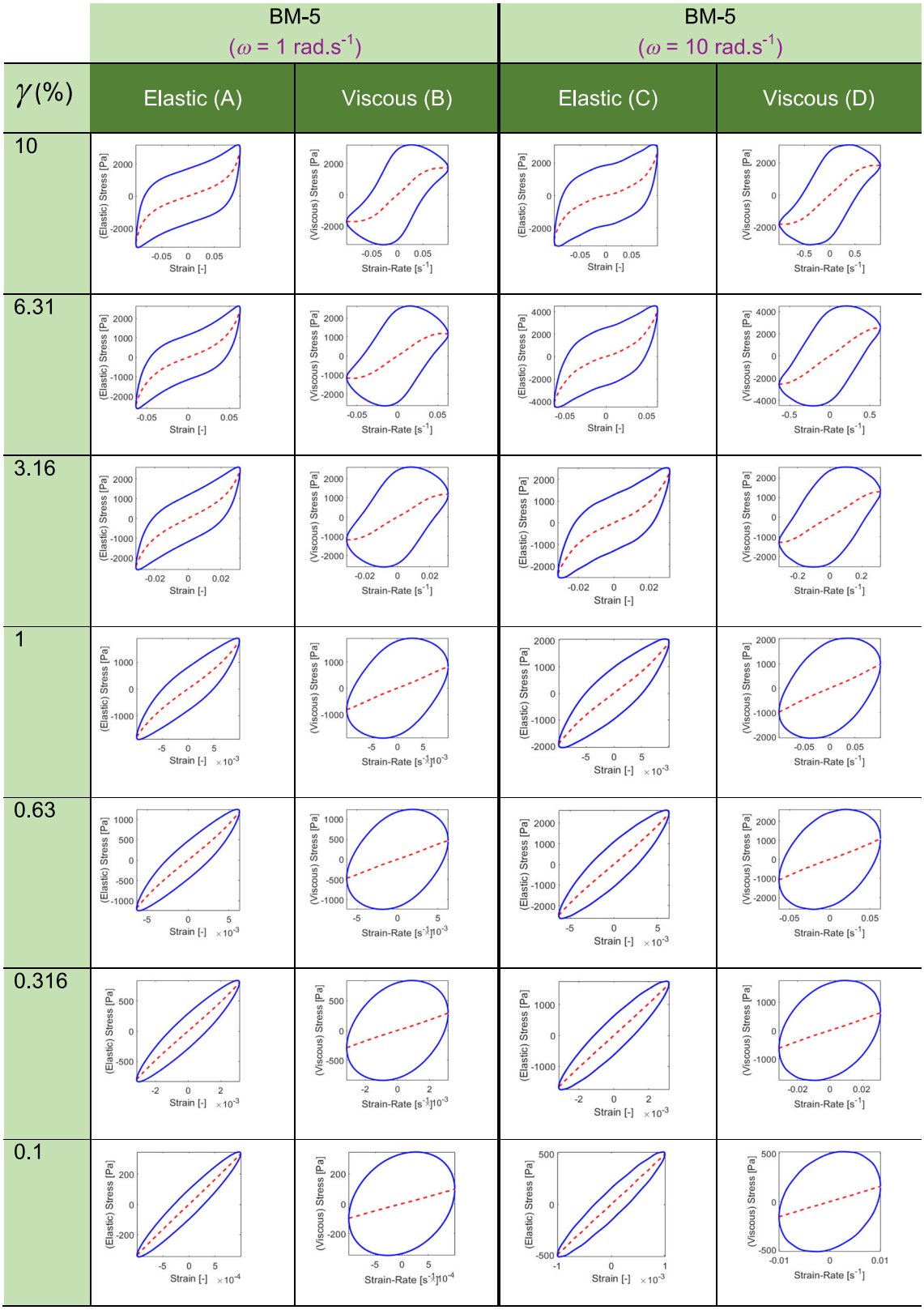

Fig. 3 Elastic (columns A and C) and viscous (columns B and D) Lissajous–Bowditch curves of benchmark prototype BM-5. The columns A and B refer to $\omega = 1\,\mathrm{rad\,s^{-1}}$, and the columns C and D to $\omega = 10\,\mathrm{rad\,s^{-1}}$. The rows represent the intracycle response, i.e., the instantaneous elastic or viscous stress as a function of instantaneous strain or strain rate, corresponding to a distinct strain amplitude

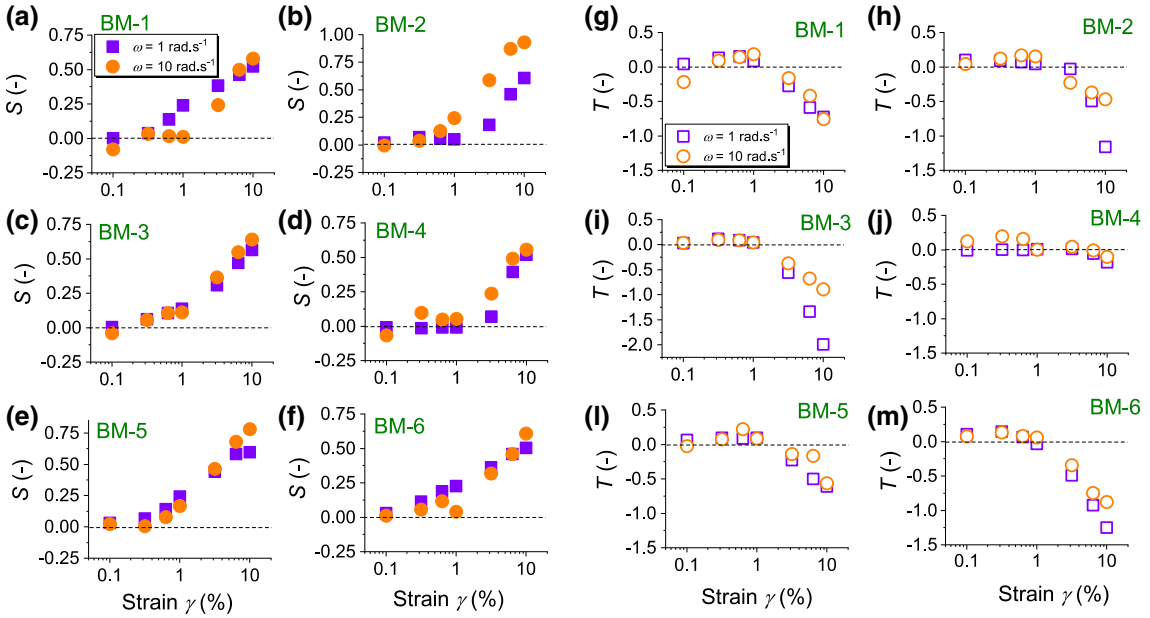

Fig. 4 Strain stiffening ratio (left panel, filled symbols) and shear thickening ratio (right panel, open symbols), S and T, respectively, as a function of imposed strain amplitude. The measurements were performed at $\omega = 1$ rad s^{-1} (squares) and $\omega = 10$ rad s^{-1} (circles), as indicated in the legends of the subfigures (**a**, **g**). The sample codes are explained in Table 1

with the yield stress, affect their rubbing or pick-up features [29]. Based on Fig. 2b, the intrinsic elastic potential, i.e., G_0', showed two distinct trends. BM-2, BM-4, and BM-5 possess a higher crystal network elastic energy, compared to BM-1, BM-3, and BM-6. As noted in the previous Section, the quantity G_0' is larger at the higher angular frequency of 10 rad s^{-1}. This is expected since higher elastic energy is stored at the higher intracycle shear rates. One important observation was the different extents of strain softening corresponding to different benchmarks, as shown in Fig. 2c. Ozkan et al. [30] showed that the extent of strain softening of different skin/hair care gels bears a dependence on the underlying polymer constituents. When measured in rough geometries, the strain-softening behavior becomes independent of the formulation at very high strain amplitudes ($> 100\%$). We see an identical behavior for the lipsticks here, but roughly at an order of magnitude before. Nonetheless, the stress tolerance of the lipsticks (Fig. 2a), based on the values of τ^*, does not show an identical qualitative trend as with G_0'. Intracycle elastic strain hardening or viscous shear thinning is related to the third harmonic contribution and is observed in similarly layered systems, i.e., biopolymer gels [20,37,46,47] and ex vivo human skin and aged internal human vocal fold tissues [41,42,45]. However, these trends are in contrast to the nonlinear responses of synthetic entangled polyacrylamide systems [36]. A previous LAOS study on composite skincare formulations reported viscous Lissajous plots [28]. However, these tests were carried out at $\omega = 50$ rad s^{-1} and in the range of 1–600% strain amplitude using an ARES-G2 strain-controlled rheometer. Despite that, intracycle viscous shear thinning was observed irrespective of the formulation in the nonlinear regime, in agreement with the current study. The unique rheological observations made here cannot be directly compared with those in past studies, due to the lack of suitable data in the literature. This is especially true for the Lissajous curves observed between 20 and 100% strain amplitudes (data not shown), which represent the post-crossover region. The curves manifest a wide range of irregularities, including non-reproducible fluctuations in the decayed instantaneous elastic and viscous stress response. Macroscopic fractures were also observed for all the benchmark lipsticks after completion of the strain amplitude sweeps, i.e., after the maximum imposed strain amplitude of 100%.

From the perspectives of the customers, much depends on a myriad of factors, including climatic conditions, stages of physical development, geographical location, economic situations, amongst others. This was exclusively highlighted in our recent article [11], with a proposed indication of sensory features based on the thermomechanical properties of the same benchmark lipsticks. Although rheology brings out the best in terms of apparent strengths of textures, it does not facilitate a careful appraisal of either the demonstrative assessments or the subtle morphological characteristics [30]. In this regard, a systematic sensorial analysis of the rheological features evaluated by a trained panel could provide more in-depth insights [48]. Gillece et al.

[28] reported that slip, quick break, and cushion are initial-to-intermediate sensorial attributes that are most suited for association with rheology. Since we employed a rough surface geometry with sandpaper, we could majorly circumvent slip. Based on the results of the current study, we can use some of the mechanical lipstick features, i.e., the zero-strain elastic modulus or G'_0, the stress maxima or τ^*, the melting temperature from our previous study [11], and the extent of the linear viscoelastic regime, to indicate a few sensory attributes. Potential customers preferring hard textures may choose from BM-2, BM-4, and BM-5. Customers preferring soft textures may choose between BM-6 and BM-1. These are based on visual observations and the trends of both G'_0, and τ^*, as shown in Fig. 2a, b. Parameters such as the stress maximum and zero-shear rate viscosity were shown to be effective indicators of easy break and cushion sensory features of composite skincare formulations [28]. The preference of the color and the perfume differs significantly between the young and adult customers. The fragrance and the colors in the benchmark lipstick models were shown to be inconsequential in terms of affecting the thermomechanical properties [11]. Customers preferring highly deformation-tolerant lipsticks may opt between BM-1, BM-2, and BM-5. This is based on the larger extents of their linear viscoelastic regimes from strain amplitude sweeps at $\omega = 10\,\mathrm{rad\,s^{-1}}$. The natural component-based BM-2 was particularly noted for its superior temperature stability based on its high melting temperature of $\sim 75\,^{\circ}\mathrm{C}$ [11].

Besides rheological characterizations, standard tribological techniques could be employed for investigating the lubricating properties of these benchmark lipsticks. This will serve as an independent and novel future work, including studying their relation with the sensory attributes. For instance, the effects of sliding speed on the coefficient of friction, or the effects of disk speed and normal force on friction and wear, could be investigated. This will tribologically evaluate the prospects of the benchmark lipsticks, considering that these methods are crucial to lipstick performance [4]. The combined application of the LAOS technique and tribology will allow investigations at much smaller gap lengths and can be applied to very thin lipstick films. This will enable examining the physicochemical features of lipsticks, ultimately facilitating a better understanding of the transformation from the lipstick initial spreading to the post-application sensation [28]. Besides, the tribo-rheological properties could be associated with the lipstick sensorial attributes via a systematic evaluation by a trained panel.

5 Conclusions

Advanced mechanical properties of six different commercially procurable standard lipstick models were investigated under LAOS stresses. A few common trends for all the lipsticks could be noted in both the linear as well as nonlinear viscoelastic regimes. In the frequency sweeps carried out at low strain amplitudes ($< 0.1\%$), we found a dominant intracycle elastic response. The strain amplitude sweeps showed intercycle strain-softening behavior at higher strain amplitudes (between 0.1 to 10%), the extent of this behavior depending on the lipstick type. However, after the crossover point ($> 20\%$ strain amplitude), this dependence disappeared. The linear and nonlinear parameters obtained from the strain amplitude sweeps, i.e., the extent of the LVE regime, the intrinsic elastic potential, and the stress maximum, showed lipstick dependence. The magnitude of the oscillation frequency did not show a strong influence on either the qualitative or quantitative nonlinear responses. We note that with the technique employed in the current study, the LAOS measures could be quite accurately captured up to a strain amplitude of $\sim 20\%$. There are several opportunities for future investigations, such as designing an independent tribological study to examine the friction and lubricating properties or the connotation of sensory attributes to tribo-rheological parameters.

Acknowledgements Open Access funding provided by Projekt DEAL. The authors thank Dr. Sivatharushan Sivanathan, Mr. Gero Kiepe, and Dr. Thomas Kiepe from KHK, GmbH (Cologne, Germany) for donating their natural component-based benchmark lipstick BM-2. SP acknowledges the discussions with Dr. Thomas B. Goudoulas (Fluid Dynamics of Complex Biosystems, Technical University of Munich). We also wish to thank the anonymous reviewers for their valuable feedback and suggestions.

Funding The current work was funded by the Allianz Industrie Forschung (AiF) grant (Funding code: ZF4025024MD7; AiF Projekt GmbH), a strategic collaboration between KHK GmbH and the Technical University of Munich, as a part of the Central Innovation Program Initiative of the Federal Government of Germany.

References

1. Bryce, D.M.: Lipstick. In: Butler, H. (ed.) Poucher's Perfumes, Cosmetics and Soaps, pp. 213–243. Springer, Dordrecht (1993)
2. Richard, C., Tillé-Salmon, B., Mofid, Y.: Contribution to interplay between a delamination test and a sensory analysis of mid-range lipsticks. Int. J. Cosmet. Sci. **38**, 100–108 (2016). https://doi.org/10.1111/ics.12242
3. Taylor, M.S.: Stabilisation of water-in-oil emulsions to improve the emollient properties of lipstick. Ph.D. Thesis, University of Birmingham (2011)
4. Beri, A.: Wax based emulsions for use in lipstick application. Ph.D. Thesis, University of Birmingham (2015)
5. Rocha, J.C.B., Lopes, J.D., Mascarenhas, M.C.N., Arellano, D.B., Guerreiro, L.M.R., da Cunha, R.L.: Thermal and rheological properties of organogels formed by sugarcane or candelilla wax in soybean oil. Food Res. Int. **50**, 318–323 (2013). https://doi.org/10.1016/j.foodres.2012.10.043
6. Bono, A., Mun, H.C., Rajin, M.: Effect of various formulation on viscosity and melting point of natural ingredient based lipstick. In: Rhee, H.-K. (ed.) New developments and Application in Chemical Reaction Engineering: Proceedings of the 4th Asia-Pacific Chemical Reaction Engineering Symposium (APCRE '05), Gyeongju, Korea, 12–15 June 2005, pp. 693–696. Elsevier, Amsterdam (2006)
7. Goik, U., Ptaszek, A., Goik, T.: The influence of propolis on rheological properties of lipstick. Int. J. Cosmet. Sci. **37**, 417–424 (2015). https://doi.org/10.1111/ics.12213
8. Beri, A., Norton, J.E., Norton, I.T.: Effect of emulsifier type and concentration, aqueous phase volume and wax ratio on physical, material and mechanical properties of water in oil lipsticks. Int. J. Cosmet. Sci. **35**, 613–621 (2013). https://doi.org/10.1111/ics.12085
9. Tavernier, I., Doan, C.D., van de Walle, D., Danthine, S., Rimaux, T., Dewettinck, K.: Sequential crystallization of high and low melting waxes to improve oil structuring in wax-based oleogels. RSC Adv. **7**, 12113–12125 (2017). https://doi.org/10.1039/C6RA27650D
10. Liu, H., Lu, Y., Zhang, J.: A comprehensive investigation of the viscoelasticity and time-dependent yielding transition of waxy crude oils. J. Rheol. **62**(2), 527–541 (2018). https://doi.org/10.1122/1.5002589
11. Pan, S., Germann, N.: Thermal and mechanical properties of industrial benchmark lipstick prototypes. Thermochim. Acta **679**, art. no. 178332 (2019). https://doi.org/10.1016/j.tca.2019.178332
12. Dimitriou, C.J., Ewoldt, R.H., McKinley, G.H.: Describing and prescribing the constitutive response of yield stress fluids using large amplitude oscillatory shear stress (LAOStress). J. Rheol. **57**(1), 27–70 (2013). https://doi.org/10.1122/1.4754023
13. Ewoldt, R.H.: Defining nonlinear rheological material functions for oscillatory shear. J. Rheol. **57**(1), 177–195 (2013). https://doi.org/10.1122/1.4764498
14. Bae, J.-E., Lee, M., Cho, K.S., Seo, K.H., Kang, D.-G.: Comparison of stress-controlled and strain-controlled rheometers for large amplitude oscillatory shear. Rheol. Acta **52**(10–12), 841–857 (2013). https://doi.org/10.1007/s00397-013-0720-8
15. Rogers, S.A.: In search of physical meaning: defining transient parameters for nonlinear viscoelasticity. Rheol. Acta **56**(5), 501–525 (2017). https://doi.org/10.1007/s00397-017-1008-1
16. Wilhelm, M., Reinheimer, P., Ortseifer, M.: High sensitivity Fourier-transform rheology. Rheol. Acta **38**, 349–356 (1999)
17. Wilhelm, M., Reinheimer, P., Ortseifer, M., Neidhöfer, T., Spiess, H.W.: The crossover between linear and nonlinear mechanical behaviour in polymer solutions as detected by Fourier-transform rheology. Rheol. Acta **39**, 241–247 (2000)
18. Cho, K.S., Hyun, K., Ahn, K.H., Lee, S.J.: A geometrical interpretation of large amplitude oscillatory shear response. J. Rheol. **49**(2), 747–758 (2005). https://doi.org/10.1122/1.1895801
19. Hyun, K., Wilhelm, M., Klein, C.O., Cho, K.S., Nam, J.G., Ahn, K.H., Lee, S.J., Ewoldt, R.H., McKinley, G.H.: A review of nonlinear oscillatory shear tests: analysis and application of large amplitude oscillatory shear (LAOS). Prog. Polym. Sci. (Oxf.) **36**(12), 1697–1753 (2011). https://doi.org/10.1016/j.progpolymsci.2011.02.002
20. Ewoldt, R.H., Hosoi, A.E., McKinley, G.H.: New measures for characterizing nonlinear viscoelasticity in large amplitude oscillatory shear. J. Rheol. **52**(6), 1427–1458 (2008). https://doi.org/10.1122/1.2970095
21. Rogers, S.A., Lettinga, M.P.: A sequence of physical processes determined and quantified in large-amplitude oscillatory shear (LAOS): application to theoretical nonlinear models. J. Rheol. **56**(1), 1–25 (2012). https://doi.org/10.1122/1.3662962
22. Poulos, A.S., Stellbrink, J., Petekidis, G.: Flow of concentrated solutions of starlike micelles under large-amplitude oscillatory shear. Rheol. Acta **52**(8–9), 785–800 (2013). https://doi.org/10.1007/s00397-013-0703-
23. De Souza Mendes, P.R., Thompson, R.L., Alicke, A.A., Leite, R.T.: The quasilinear large-amplitude viscoelastic regime and its significance in the rheological characterization of soft matter. J. Rheol. **58**(2), 537–561 (2014). https://doi.org/10.1122/1.4865695
24. Lee, J.C.-W., Weigandt, K.M., Kelley, E.G., Rogers, S.A.: Structure–property relationships via recovery rheology in viscoelastic materials. Phys. Rev. Lett. **122**(24), art. no. 248003 (2019). https://doi.org/10.1103/PhysRevLett.122.248003
25. Donley, G.J., de Bruyn, J.R., McKinley, G.H., Rogers, S.A.: Time-resolved dynamics of the yielding transition in soft materials. J. Nonnewton. Fluid Mech. **264**, 117–134 (2019). https://doi.org/10.1016/j.jnnfm.2018.10.003
26. Rogers, S.A., Park, J.D., Lee, C.-W.J.: Instantaneous dimensionless numbers for transient nonlinear rheology. Rheol. Acta **58**(8), 539–556 (2019). https://doi.org/10.1007/s00397-019-01150-2
27. Mitsui, T., Morosawa, K., Ötake, C.: Estimation of the rate of shear encountered in topical application of cosmetics. J. Texture Stud. **2**(3), 339–347 (1971). https://doi.org/10.1111/j.1745-4603.1971.tb01010.x
28. Gillece, T., Mcmullen, R.L., Fares, H., Senak, L., Ozkan, S., Foltis, L.: Probing the textures of composite skin care formulations using large amplitude oscillatory shear. J. Cosmet. Sci. **67**(2), 121–159 (2016)

29. Pénzes, T., Csóka, I., Eros, I.: Rheological analysis of the structural properties effecting the percutaneous absorption and stability in pharmaceutical organogels. Rheol. Acta **43**(5), 457–463 (2004). https://doi.org/10.1007/s00397-004-0396-1
30. Ozkan, S., Gillece, T.W., Senak, L., Moore, D.J.: Characterization of yield stress and slip behaviour of skin/hair care gels using steady flow and LAOS measurements and their correlation with sensorial attributes. Int. J. Cosmet. Sci. **34**(2), 193–201 (2012). https://doi.org/10.1111/j.1468-2494.2012.00702.x
31. Haj-shafiei, S., Ghosh, S., Rousseau, D.: Kinetic stability and rheology of wax-stabilized water-in-oil emulsions at different water cuts. J. Colloid Interface Sci. **410**, 11–20 (2013). https://doi.org/10.1016/j.jcis.2013.06.047
32. Timm, K., Myant, C., Spikes, H.A., Grunze, M.: Particulate lubricants in cosmetic applications. Tribol. Int. **44**, 1695–1703 (2011)
33. Kusakari, K., Yoshida, M., Matsuzaki, F., Yanaki, T., Fukui, H., Date, M.: Evaluation of post-application rheological changes in cosmetics using a novel measuring device: relationship to sensory evaluation. J. Cosmet. Sci. **54**, 321–334 (2003)
34. Läuger, J., Stettin, H.: Differences between stress and strain control in the non-linear behavior of complex fluids. Rheol. Acta **49**(9), 909–930 (2010). https://doi.org/10.1007/s00397-010-0450-0
35. Pan, S., Malhotra, D., Germann, N.: Nonlinear viscoelastic properties of native male human skin and in vitro 3D reconstructed skin models under LAOS stress. J. Mech. Behav. Biomed. Mater. **96**, 310–323 (2019). https://doi.org/10.1016/j.jmbbm.2019.04.032
36. Goudoulas, T.B., Pan, S., Germann, N.: Nonlinearities and shear banding instability of polyacrylamide solutions under large amplitude oscillatory shear. J. Rheol. **61**(5), 1061–1083 (2017). https://doi.org/10.1122/1.4998931
37. Goudoulas, T.B., Pan, S., Germann, N.: Double-stranded and single-stranded well-entangled DNA solutions under LAOS: a comprehensive study. Polymer **140**, 240–254 (2018). https://doi.org/10.1016/j.polymer.2018.02.061
38. Malhotra, D., Pan, S., Rüther, L., Goudoulas, T.B., Schlippe, G., Voss, W., Germann, N.: Linear viscoelastic and microstructural properties of native male human skin and in vitro 3D reconstructed skin models. J. Mech. Behav. Biomed. Mater. **90**, 644–654 (2019). https://doi.org/10.1016/j.jmbbm.2018.11.013
39. Höfl, S., Kremer, F., Spiess, H.W., Wilhelm, M., Kahle, S.: Effect of large amplitude oscillatory shear (LAOS) on the dielectric response of 1,4-cis-polyisoprene. Polymer **47**(20), 7282–7288 (2006). https://doi.org/10.1016/j.polymer.2006.03.116
40. Chen, M.H., Wang, L.L., Chung, J.J., Kim, Y.-H., Atluri, P., Burdick, J.A.: Methods to assess shear-thinning hydrogels for application as injectable biomaterials. ACS Biomater. Sci. Eng. **3**(12), 3146–3160 (2017). https://doi.org/10.1021/acsbiomaterials.7b00734
41. Chan, R.W.: Nonlinear viscoelastic characterization of human vocal fold tissues under large-amplitude oscillatory shear (LAOS). J. Rheol. **62**(2), 695–712 (2018). https://doi.org/10.1122/1.4996320
42. Lamers, E., van Kempen, T.H.S., Baaijens, F.P.T., Peters, G.W.M., Oomens, C.W.J.: Large amplitude oscillatory shear properties of human skin. J. Mech. Behav. Biomed. Mater. **28**, 462–470 (2013). https://doi.org/10.1016/j.jmbbm.2013.01.024
43. Goudoulas, T.B., Germann, N.: Phase transition kinetics and rheology of gelatin-alginate mixtures. Food Hydrocolloids **66**, 49–60 (2017). https://doi.org/10.1016/j.foodhyd.2016.12.018
44. Szopinski, D., Luinstra, G.A.: Viscoelastic properties of aqueous guar gum derivative solutions under large amplitude oscillatory shear (LAOS). Carbohydr. Polym. **153**, 312–319 (2016). https://doi.org/10.1016/j.carbpol.2016.07.095
45. Alghooneh, A., Razavi, S.M.A., Kasapis, S.: Classification of hydrocolloids based on small amplitude oscillatory shear, large amplitude oscillatory shear, and textural properties. J. Texture Stud. (2019). https://doi.org/10.1111/jtxs.12459
46. Sun, W.-X., Huang, L.-Z., Yang, Y.-R., Liu, X.-X., Tong, Z.: Large amplitude oscillatory shear studies on the strain-stiffening behavior of gelatin gels. Chin. J. Polym. Sci. (Engl. Ed.) **33**(1), 70–83 (2015). https://doi.org/10.1007/s10118-015-1559-5
47. John, J., Ray, D., Aswal, V.K., Deshpande, A.P., Varughese, S.: Dissipation and strain-stiffening behavior of pectin-Ca gels under LAOS. Soft Matter **15**(34), 6852–6866 (2019). https://doi.org/10.1039/c9sm00709a
48. Meilgaard, M.C., Civille, C.V., Carr, B.T.: Sensory Evaluation Techniques, 4th edn, pp. 7–24. CRC Press, Boca Raton (2007)